Journal of Scientific Research and Reports

Volume 30, Issue 4, Page 61-76, 2024; Article no.JSRR.113723
ISSN: 2320-0227

Development and Characterization of Nano-Chitosan-Polyvinyl Alcohol-Glycerol -Chlorhexidine Films for Wound Healing Applications

Rosemol Jacob M. [a,b], Amruth P. [a,b], Preethy Treesa Paul [a,b] Jean Mary Joy [a,b], Visnuvinayagam S. [c], Pavan Kumar Dara [d], R. Anandan [a] and Suseela Mathew [a*]

[a] Biochemistry and Nutrition Division, ICAR-Central Institute of Fisheries Technology, Cochin, 682029, Kerala, India.
[b] Faculty of Marine Sciences, Cochin University of Science and Technology, Cochin, 682022, Kerala, India.
[c] Microbiology, Fermentation and Biotechnology Division, ICAR-Central Institute of Fisheries Technology, Cochin, 682029, Kerala, India.
[d] Department of Biotechnology, SRM Institute of Science and Technology, Tamil Nadu, 603203, India.

Authors' contributions

This work was carried out in collaboration among all authors. All authors read and approved the final manuscript.

Article Information

DOI: 10.9734/JSRR/2024/v30i41890

Open Peer Review History:
This journal follows the Advanced Open Peer Review policy. Identity of the Reviewers, Editor(s) and additional Reviewers, peer review comments, different versions of the manuscript, comments of the editors, etc are available here: https://www.sdiarticle5.com/review-history/113723

Original Research Article

Received: 16/12/2023
Accepted: 22/02/2024
Published: 27/02/2024

**Corresponding author: E-mail: suseela1962@gmail.com;*

ABSTRACT

The process of wound healing is intricate and dynamic, requiring advanced medical care for a speedy recovery. Currently available semi-permeable wound dressings fall short in efficiently absorbing excess wound exudates to facilitate moist wound care, a crucial factor for promoting effective wound healing. Additionally, efforts have been made to enhance the antibacterial properties of wound dressings by incorporating antimicrobials into films. In this study, films were development using nanochitosan-polyvinyl alcohol-glycerol-chlorhexidine (NC-PVA-GLY-CLX) for applications in wound healing. The dressings were subjected to various characterizations, including UV-Visible spectrometry, Fourier Transform Infrared Spectroscopy, Scanning Electron Microscopy, Thermogravimetric analysis, and X-ray diffraction pattern. Furthermore, the resulting film dressings underwent evaluation for their bactericidal properties. The findings indicated that the incorporation of chlorhexidine into the films has positively influenced the fluid holding capacity and the active period of the dressing, creating a favourable environment for effective wound healing.

Keywords: Chlorhexidine; nanochitosan; chitosan nanoparticles; antimicrobial activity.

1. INTRODUCTION

The wound healing process is intricate and dynamic pathophysiological process, necessitating advanced medical interventions for effective recovery and well-being [1, 2]. Film-based dressings play a pivotal role in wound care, demonstrating significant potential in treating acute to moderate wounds [3]. Particularly, film-based dressings, known for their superior flexibility, exhibit promising applications, especially in periodontal wound care [4]. However, existing semi-permeable films often fall short in moist wound care [5]. Therefore, the development of wound care devices capable of absorbing exudates is highly favoured. Ideal wound dressings should possess crucial attributes such as bacterial permeability, gaseous exchange, sufficient water vapor transmission (WVTR), biocompatibility, and biodegradability [6] for effective healing.

Various natural polymers are extensively explored in the development of wound dressings, incorporating potential cross-linkers and plasticizers to achieve optimal techno-functional attributes suitable for wound dressing applications [7, 8]. Among these polymers, chitosan stands out due to its viscoelastic, thermal, rheological, physical, physico-mechanical, and structural properties. Chitosan, a cationic (positively charged) natural polymer derived from marine shrimps and crab shells, exhibits non-immunogenicity, non-cytotoxicity, antibacterial capabilities [9] biodegradability, and biocompatibility [10], making it optimal for wound healing applications. Chitosan's unique properties arise from the presence of primary amines along its backbone, allowing it to form complexes with anionic counterparts for modulated bio-functionality optimal for wound healing [11]. Polyvinyl alcohol (PVA), when combined with chitosan, enhances film properties, offering good tensile strength, flexibility, biodegradability, and biocompatibility [12]. Glycerol, a non-volatile polyol, acts as a plasticizer in film-forming solutions to enhance the flexibility of films [13].

Chlorhexidine (CLX), a gold standard antiseptic agent, exhibits effective antibacterial properties due to its amphipathic symmetrical structure. Its bacteriostatic and bactericidal actions make it a prominent candidate for wound healing applications [14]. Incorporating CLX into chitosan films enhances bactericidal properties and enables sustained release from the polymeric matrix, promoting reduced cytotoxicity for fibroblast cells. The protective barrier provided by chitosan facilitates tissue regeneration, while chlorhexidine prevents infections, expediting the healing process [15]. Nanoparticles synthesized from natural polymers, such as nanochitosan, gain prominence due to their small size and large surface-to-volume ratio [16]. Nanochitosan, produced through ionic gelation, exhibits reproducibility and nano size particles with a highly positive surface charge [9]. This study explores the synthesis of nano-sized chitosan reinforced with chlorhexidine, plasticized with glycerol, and cross-linked with PVA to create bioactive films for wound healing applications. The *in vivo* studies were carried out in male Wistar rats [17] and data not presented in this paper. The synergistic effects of chitosan, PVA, and CLX are comprehensively examined for their functional and bioactive properties through various characterizations, including UV-visible

spectroscopy, Fourier Transform Infrared Spectroscopy (FTIR), Scanning Electron Microscopy (SEM), Thermogravimetric analysis **(**TGA), and X-ray diffraction pattern (XRD). The films are further evaluated for their bactericidal properties in a dynamic wound environment.

2. MATERIALS AND METHODS

2.1 Materials

Chitosan (Low molecular weight) with a deacetylation level of 75% and polyvinyl alcohol (PVA) were acquired from Sigma-Aldrich Chemical Pvt Limited, located in Bangalore, India. Glycerol and all other substances utilized in the current investigation were of either analytical grade (AR) or guaranteed grade (GR). Chlorhexidine base gifted from AB Shetty Dental College, Mangalore.

2.2 Preparation of Nano Chitosan

1% chitosan was used to prepare nanochitosan using sodium tripolyphosphate (STPP), which was added drop by drop into chitosan kept on a magnetic stirrer and solution was stirred for 1 h. The solution was subjected to ultra-sonication for the production of nanochitosan [18].

2.3 Casting of Films

Polyvinyl alcohol and 0.05% chlorhexidine were introduced to the prepared nanochitosan solution, and the mixture was stirred continuously until a transparent solution was achieved. The fully dissolved solution was then poured onto a tray and left overnight in a hot air oven at 55°C to produce a chlorhexidine nanochitosan film [18].

2.4 Characterisation of Nanochitosan Film Incorporated with Chlorhexidine

2.4.1 Particle size and zeta potential

The determination of particle size, polydispersity index (PDI), and zeta potential for nanochitosan solutions, nanochitosan with added chlorhexidine, and chlorhexidine (0.05%) was conducted employing dynamic light scattering analyses (DLS). These measurements were performed using a Zeta Sizer Nano Series instrument from Malvern in Worcestershire, UK.

2.4.2 UV- Vis spectra

The UV–Vis spectra of nanochitosan solutions, nanochitosan with the integration of chlorhexidine, and chlorhexidine (0.05%) solutions were examined within 200-700 nm wavelength range. This analysis was performed using a double beam spectrophotometer (Shimadzu, UV-1800, Japan). A graph illustrating absorbance against wavelength was generated to obtain the absorption spectra.

2.4.3 FTIR

To identify specific chemical groups in the material Fourier Transform Infrared Spectroscopy was carried out. The FTIR spectra of the films were inspected using an FTIR spectrometer (Nicolet iS50) across the wavenumber range of 4000 to 500 cm^{-1}, with 64 scans at a resolution of 4 cm^{-1}.

2.4.4 SEM

The surface characteristics of the films were assessed through SEM images captured using a Jeol 6390LA/ OXFORD XMX N, a scanning Electron Microscope equipped with an Energy Dispersive X-Ray Spectroscope (SEM-EDAX) operating at an acceleration voltage ranging from 0.5 to 30 kV. Various magnifications were employed to capture the surface morphologies.

2.4.5 XRD pattern

The films were subjected to X-ray powder diffraction analysis using a Bruker D8 Advance diffractometer. Cu Kα radiation (40 kV, 80 mA) was employed as the X-ray source. The XRD patterns of the samples were recorded over the 2θ range of 3-10 initially and the final scanning at 10–80, utilizing a fixed time mode at room temperature and a scanning rate of 4˚ min−1.

2.4.6 Thermal characteristics

The specimens underwent a temperature increase from 40°C to 750°C at a heating rate of 10°C/min, utilizing the thermogravimetric analyzer TGA-DTA Perkin Elmer STA6000, specifically the Perkin Elmer Diamond model. The analysis involved the examination of the films through DTG (derivative thermo-gravity) and DTA (differential thermal analysis)

2.4.7 Moisture content

Film specimens measuring approximately 2 x 2 cm were precisely weighed on a dried petri plate and then positioned in a hot air oven (Rotek Instruments, B & C Industries, Cochin, and

India). The oven's temperature was maintained at 105 ± 5 ˚C for a duration of 24 hours. Subsequently, the petri plates were taken out from the hot air oven and allowed to cool within desiccators containing silica gel at room temperature. This process of heating and cooling was iterated until a consistent weight was attained. The determination of the total moisture content was conducted utilizing the equation provided below [19].

$$\text{Moisture Content}(\%) = \frac{W1 - W2}{W1} X\ 100$$

Where, W1 = Initial dry weight of the sample; W2 = Final dry weight of the sample

2.4.8. Film solubility

The assessment of film pseudo exudate fluid solubility (PEF) was conducted by determining the percentage of dissolved dry matter after immersing film samples. Each film variant (1 cm X 1 cm) underwent an initial drying at 60 °C for 2 hours to establish the initial dry matter (W1). Subsequently, each film was placed in 5 mL of PEF within a petri plate and stirred gently for 24 hours. After this period, the film specimens were taken out, and their undissolved final dry weight (W2) was determined following 24 hours of drying in an oven set at 105 °C [20]. The solubility of the sample was calculated using the following formula.

$$\text{Solubility}\ (\%) = \frac{W1 - W2}{W1} X\ 100$$

Where, W1 = Initial dry weight of the sample; W2 = Final dry weight of the sample

2.4.9 Swelling Index

The swelling experiments were conducted using film strips measuring 1 × 1 cm, which were immersed in pseudo exudate fluid. The PEF composition consisted of 2% bovine serum albumin, 0.02 M calcium chloride, 0.4 M sodium chloride, and 0.08 M trismethylamine in deionized water, adjusted to pH 7.5. The weight change of the hydrated films was measured at 15 minute intervals for a duration of 150 minutes. After hydration, excess fluids on the film surface were carefully blotted with tissue paper, and the films were promptly weighed using an electronic balance [7].

$$\text{Swelling Index}\ (\%) = \frac{Ws - Wd}{Wd} X100$$

Where, W_d is dry weight of films; Ws denotes weight of film after swelling

2.4.10 Antibacterial property

In current study, the wound dressing's ability to combat bacterial infections was investigated by testing it against common gram-positive and gram-negative bacteria typically found in wound infections. To ensure quality control, *Escherichia coli*, a gram-negative bacterium known for causing pus formation in wounds, was chosen as a representative strain, specifically the ATCC 25922 strain. Furthermore, the antibacterial efficacy of the dressing was evaluated against Methicillin-Resistant *Staphylococcus aureus* (MRSA), a multidrug-resistant gram-positive bacterium, with ATCC 43300 chosen as the specific strain for assessment.

2.4.10.1 Diffusion assay

The initial assessment of antibacterial activity relied on inhibiting bacterial growth on agar plates. This involved placing the membrane over a Mueller Hinton II Agar (Cation-Adjusted) plate coated with a bacterial culture. The plates were prepared, dried, and then spread with a 0.5 McFarland standard concentrated bacterial suspension, as outlined by Visnuvinayagam et al. [21]. After 24 hours, the absence of bacteria clearance beneath the film indicated the presence of antimicrobial activity in the film.

2.4.10.2 Modified Growth Inhibition Assay

To assess the antibacterial efficacy of the film, a modified analysis of growth inhibition was performed. Small film pieces were weighed, and 15 mg of the film was placed into triplicate wells of a 96-well plate. Each well received Mueller Hinton Broth II (Cation-Adjusted) (MHB) (100 µl), followed by the addition of 10 µl of bacterial culture (approximately 5 X 10^{-5} CFU/mL) to each well, excluding the negative control wells (also in triplicate). In the positive control wells, no film was introduced. Optical density (OD) was measured every two hours, and OD values were adjusted by subtracting the initial OD value at 0 hours to eliminate background noise or errors [22].

2.5 Statistical Analysis

The experimentations were conducted in triplicate, and the reported values represent averages with standard deviations. Collected

data for various measured parameters were presented and subjected to analysis using the t-test with a significance level at 5% using SAS 9.3

3. RESULTS AND DISCUSSION

3.1 Particle Size

The characterization of particle size distribution holds paramount significance in determining the functionality of a substance, offering insights into the average particle size. Table 1 provides a detailed account of the average particle size observed in the film-forming solutions. Particularly in applications such as drug delivery systems, a preference for smaller particle sizes is commonly acknowledged [23]. The polydispersion index served as a metric for assessing the distribution or uniformity of particle sizes within a given sample. A lower PDI value signified a more uniform distribution, indicating a narrower range of particle sizes. The diminutive size of the particles resulting from the chitosan and STPP reaction can be attributed to the utilization of low molecular weight chitosan in this study. Hydrogen bonds developed by the amino and hydroxyl groups of chitosan, in conjunction with the hydroxyl groups and oxygen atoms of water influences the chitosan's charge stability. The strength of the hydrogen bond attraction plays a pivotal role in the propensity of these particles to agglomerate [24]. Additionally, the addition of STPP increased the ionic strength and overall stability of particles being linked by their ions, resulting in aggregate formation [25]. The reduced particle size of NC-CLX is attained through the stabilizing influence of chitosan.

3.2 Zeta Potential

The zeta potential characterizes the potential difference between the dispersal medium and the fluid layer adhering to the charged nanocrystals in a colloidal system. Chitosan, being a polycationic electrolyte with amino groups, imparts a positive zeta potential to the chitosan nanoparticles due to the formation of hydrogen bonds between the amino and hydroxyl groups and the hydroxyl groups or oxygen atoms in water. The presence of STPP decreases the zeta potential of the nanoparticles, as increased crosslinking occurs, leading to the neutralization of protonated amino groups by STPP anions [26].In the nanochitosan film-forming solution, the cationic chlorhexidine is affixed through TPP, a poly anionic electrolyte with phosphate groups. Upon addition of chlorhexidine, the positive charge on the chitosan particle surface diminishes gradually (as evidenced from the Table 1). This reduction occurred as both intermolecular and intermolecular cross-links form among chlorhexidine, STPP groups, and the amino groups of low molecular weight chitosan [24]. Zeta potentials of the nanoparticles beyond +30 mV or below -30 mV are deemed stable in colloidal suspension systems [27].

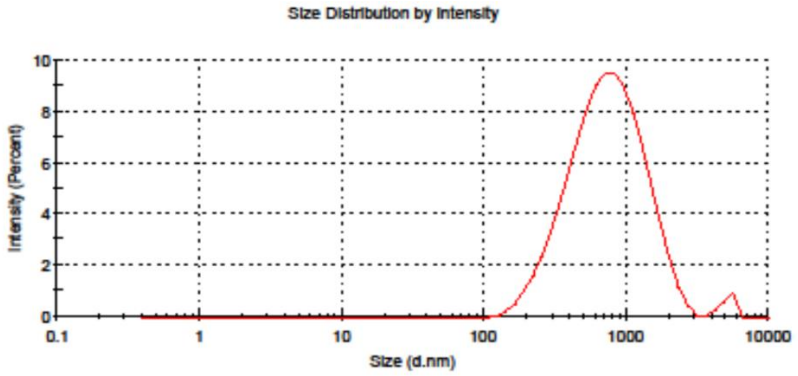

Fig. 1. Particle size of Nanochitosan in solution

Table 1. Particle size, PDI and zeta potential of the formulations

Sl. No.	Sample Name	Particle size (d.nm)	Poly dispersion index (PDI)	Zeta potential (mV)
1.	Chitosan	1989± 2.64	0.55±0.03	54.05± 1.00
2.	Nanochitosan (NC)	528.57±2.31	0.40 ±0.04	52.03± 2.00
3.	Chlorhexidine (CLX)	478.77±2.85	0.23 ±0.02	48.87±2.00
4.	Nanochitosan Chlorhexidine (NC- CLX)	319.07± 1.01	0.35±0.02	45.20±0.98

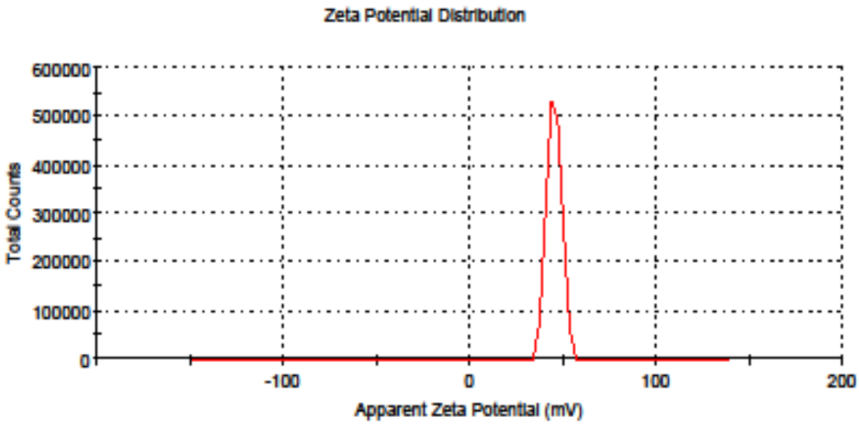

Fig. 2. Zeta potential of Nanochitosan formulations

3.3 UV-Visible Spectra

The utilization of UV–Vis spectra for characterization is favoured due to its straightforward operation and the clarity of results it provides. The UV-Vis absorption spectra, depicted in Fig 3, illustrated nanochitosan, chlorhexidine, and nanochitosan-reinforced chlorhexidine film-forming solutions. Nanochitosan exhibited a broader peak at 289 nm, while chlorhexidine displayed a distinct absorption peak at 291 nm. In the nanochitosan-chlorhexidine combination, the chlorhexidine peak at 291 nm merged with the nanochitosan peak, indicating a combination. The introduction of the new compound was evident from the UV spectrum results [28]. The merging of absorption peaks from both chitosan and chlorhexidine in the UV-Visible spectrum and the shift broadening at 291 nm suggested the successful incorporation of chlorhexidine into the chitosan solution. This indicated a proper combination of the two components in the reaction system [29].

3.4 FTIR

Fourier transform infrared spectroscopic analysis imparts insights into the functional properties, establishing correlations between functional groups and the structure of the blended film. The spectrum revealed the characteristic absorption band of nanochitosan at 3270 cm^{-1}, indicative of the –NH group in chitosan, widened by physical interactions with TPP. Strong peaks at 2939 cm^{-1}, 1646 cm^{-1}, 1561 cm^{-1}, 1328 cm^{-1}, and 1037 cm^{-1} signify asymmetrical and symmetrical stretching in CH_2 groups, NH_3^+ stretching, C=O stretching in amides, NH bending, and OH in-plane bending in alcohols, and P=O stretching, consistent with the findings of Vijayalakshmi et al. [30]. The peak at 1142 cm^{-1} indicated overlapping of C–O stretching in polysaccharide and the formation of chitosan nanoparticles due to interactions between ammonium and phosphate ions in chitosan nanoparticles [30].In the FTIR spectrum of chlorhexidine (CLX), characteristic bands at 1640 cm^{-1} signified the double bond C=N-H stretching vibration, while bands at approximately 1532 cm^{-1} and 1400 cm^{-1} correspond to aromatic C=C stretching modes. Peaks at 2923$cm^{-1}$and 2864 cm^{-1} attributed to CH_2CH stretching in methylene groups of CLX [15]. Overlapping of absorption bands between chitosan and chlorhexidine occurred, resulting in increased intensity, notably in the 3750–2750 cm^{-1} region [32].

3.5 SEM

Scanning electron microscopy was conducted to elucidate the intricate surface topography of the film specimens. Micrographs of nanochitosan films (Fig 5. a) unveiled the presence of rod-like structures. The film surfaces exhibited a notable smoothness and homogeneity, devoid of pores, cracks, or air bubbles, a consequence of the meticulous drying process (solvent casting). The conspicuous absence of voids or cracks in the film points to the application of optimal temperatures during film preparation (< 80°C). Noteworthy was the absence of agglomerations in nanochitosan films, affirming the uniform dispersion of component particles, as highlighted in the study by Zolfi et al. [32]. The findings aligned with prior research, notably the rod-like structures documented by Vijayalakshmi et al. [30].Upon the introduction of chlorhexidine into the films, a discernible alteration in surface appearance

manifested with the emergence of flake-like structures interspersed among the nano-rods. These distinct rod-like nanostructures offer a nuanced avenue for bespoke applications, particularly in sustained drug delivery scenarios where the elongated shape may confer advantages in terms of enhanced penetration or interaction with target cells.

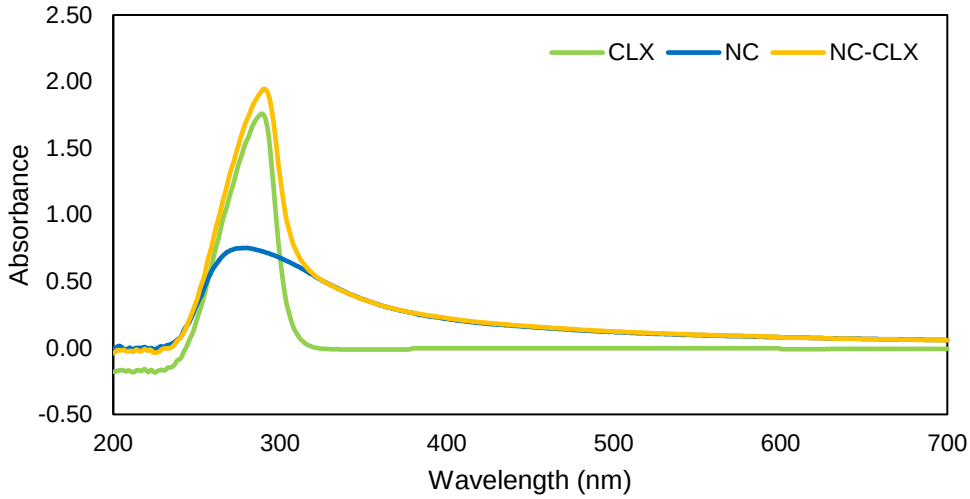

Fig. 3. UV-Visible spectra of formulations

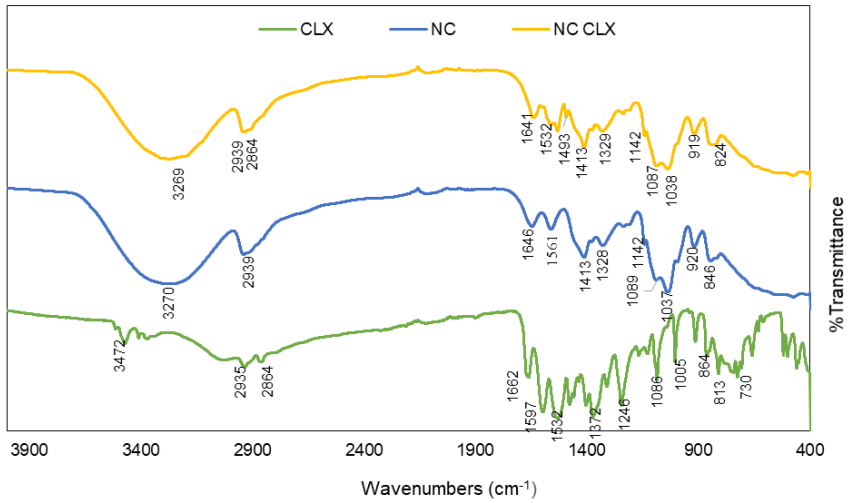

Fig. 4. FTIR spectrum of chlorhexidine, nanochitosan and nanochitosan chlorhexidine

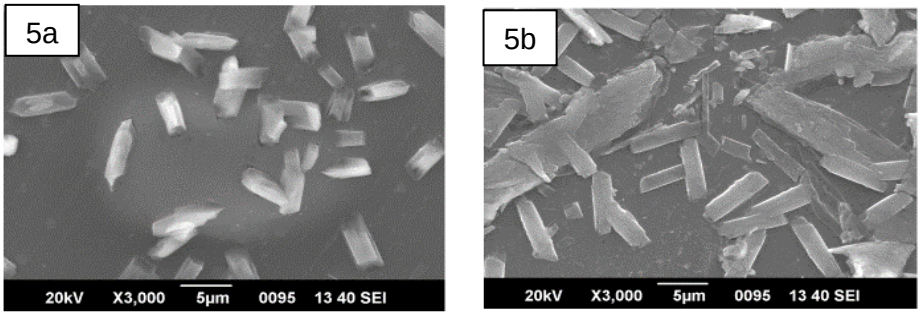

Fig. 5a. Nanochitosan and 5b.Nanochitosan Chlorhexidine film

3.6 XRD

The application of X-ray diffraction analysis served as a non-invasive analytical method for discerning modifications in the crystalline attributes, providing profound insights into crystalline phase identification, chemical composition, crystallographic structure and physical properties of materials. Consequently, a meticulous examination of the X-ray diffraction patterns of the fabricated membranes was undertaken, acknowledging the pivotal role played by the crystalline-to-amorphous ratio in comprehending the membrane development during gelation, as underscored by Vinodhini et al. [33].

The X-ray diffraction pattern of the nanochitosan film, depicted in Fig 6 displayed a diffractogram characterized by a broad peak around 2θ=19.6º. This broadening of peaks is a result of the deformation of crystalline regions due to the heightened packing of chitosan chains through ionic crosslinking. While the original chitosan molecules exhibited a certain regularity conducive to the formation of crystalline regions, crosslinking with sodium tripolyphosphate led to a diminished crystallinity of chitosan. This reduction is ascribed to the distortion of hydrogen bonds in the original chitosan caused by the substitution of hydroxyl and amino groups, effectively disrupting the orderly packing of chitosan chains and resulting in the formation of amorphous nanochitosan. Furthermore, the absence of prominent peaks at 2θ= 8.4º and 8.6º (attributable to a dispersion effect) signifies the utilization of a low concentration of chlorhexidine (CLX) (< 0.05%) in the films [30]. The presence of STPP in polymeric blends is indicated by the 2θ = 34.26º peak [25].

3.7 TGA

Thermogravimetric analysis was employed to explore the impact of temperature variations on the mass loss of the films, providing reliable insights into polymer degradation concerning temperature, decomposition temperature, and residual content under a nitrogen atmosphere, as documented by Ma et al. [34]. In the case of the nanochitosan film, degradation and weight loss were observed at rates of 3.057%/min at 185.32°C, 4.068%/min at 270.68°C, 2.5%/min at 380.43°C, 4.8%/min at 480.42°C, and 2.1%/min at 480.42°C. The primary degradation transpired within the temperature range of 184–400 °C, with the maximum weight loss rate occurring at 270 °C. Notably, Meera et al.[35] indicated that the decomposition of the principal polymeric chains of chitosan commences at 160°C, and beyond 450 °C, thermal degradation is attributed to the cross-linkages in nanochitosan [36].The modification of the nanochitosan film with the cationic drug chlorhexidine resulted in an increased number of decomposition steps. The initial degradation commenced at 74.13°C with a decomposition rate of 1.866%/min, possibly attributable to film dehydration or the removal of residual solvent [37]. The maximum weight loss occurred between 160-400°C, with decomposition rates of 3.06%/min at 229.54°C, 5.97 %/min at 270.44°C, and 2.19 %/min at 376.78°C. Additional thermal degradation events were observed at rates of 3.02 %/min at 499.48°C and 3.24%/min at 558.37°C, indicating the thermal stability of the resultant films.

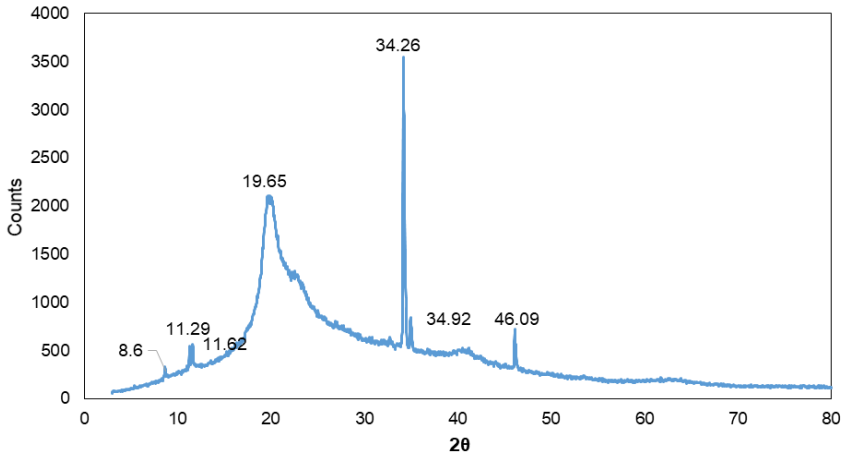

Fig. 6. XRD pattern of nanochitosan chlorhexidine film

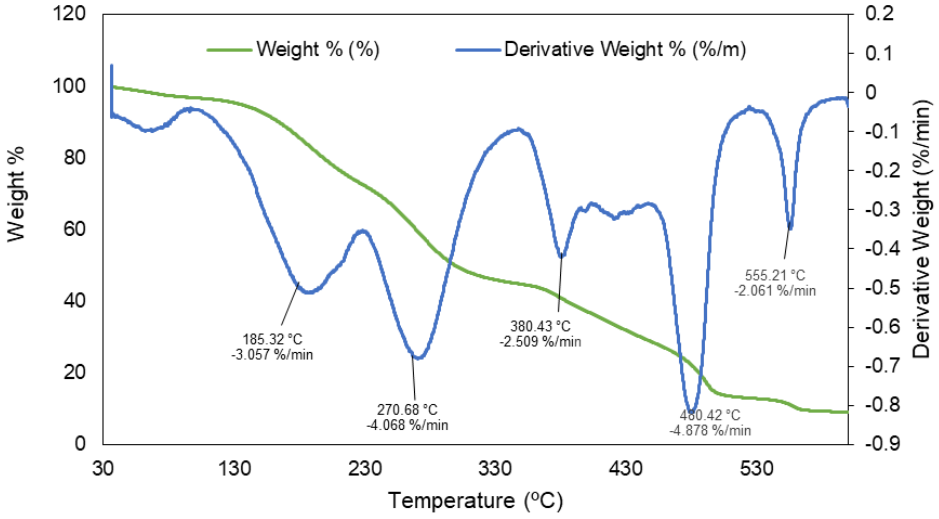

Fig. 7a. DTG of Nanochitosan Film

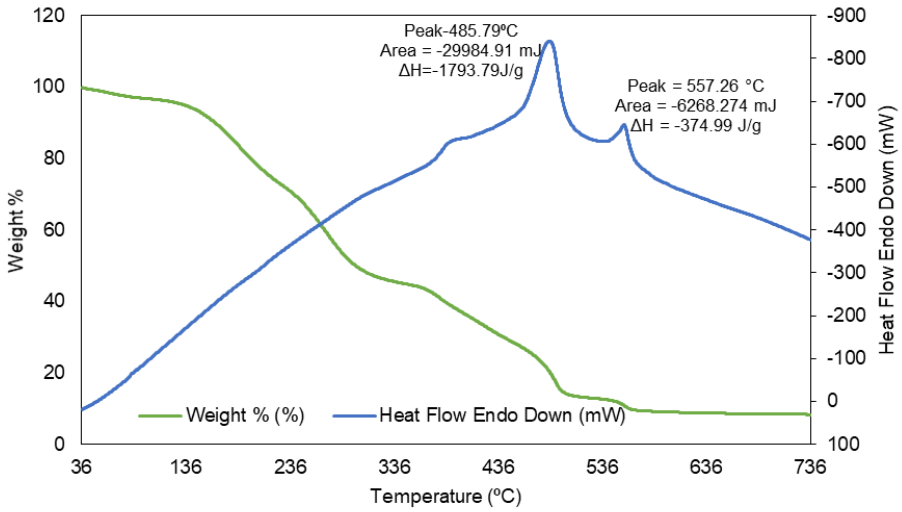

Fig. 7b. DTA of nanochitosan film

3.8 Functional Properties

3.8.1 Moisture Content (MC)

In the realm of biomedical applications for polymeric films, a pivotal aspect that demands meticulous consideration is the moisture content. Its significance is particularly pronounced in wound healing applications, exerting direct influence on the microenvironment of the wound and intricately shaping various physiological processes essential for effective wound healing [38]. Although both chitosan and PVA possess hydrophilic components, their distinct affinities and interaction capacities with water are noteworthy. The moisture content assumes the role of a modifier, significantly impacting the mechanical properties of the films [39]. According to the findings, nanochitosan films exhibited a higher moisture content, registering at 35.33±2.67 % and the results were in agreement with the study of Chopra et al., [40]. A substantial decrease to 22.44±2.03 % was evident in the moisture content of the film upon the addition of chlorhexidine, an amphipathic molecule featuring both hydrophilic and hydrophobic groups [41]. Maintaining an optimal level of moisture in the wound bed, rather than fostering a dry

environment, proves conducive to wound healing. This approach prevents tissue dehydration and subsequent cell death, fosters angiogenesis, and facilitates the removal of dead tissue, thereby promoting an environment conducive to effective wound healing [42].

3.8.2 Film solubility

Film dressings, characterized as thin transparent polymeric sheets, create a conducive environment for moist wound healing [43]. Notably, a substantial decrease in solubility was evident in pseudo exudate fluid during film solubility studies, indicating resilience to fluids. This reduction in film solubility signified the stability and resistance of the formulation to water [44]. The incorporation of chlorhexidine led to a significant reduction in solubility in pseudo exudate fluid, decreasing from 25.27±0.70% to 12.96±0.73% consistent with these studies by Abdul-Rahman and Abas [45] revealed a similar decrease in solubility values for chitosan film upon the addition of supporting substances. This

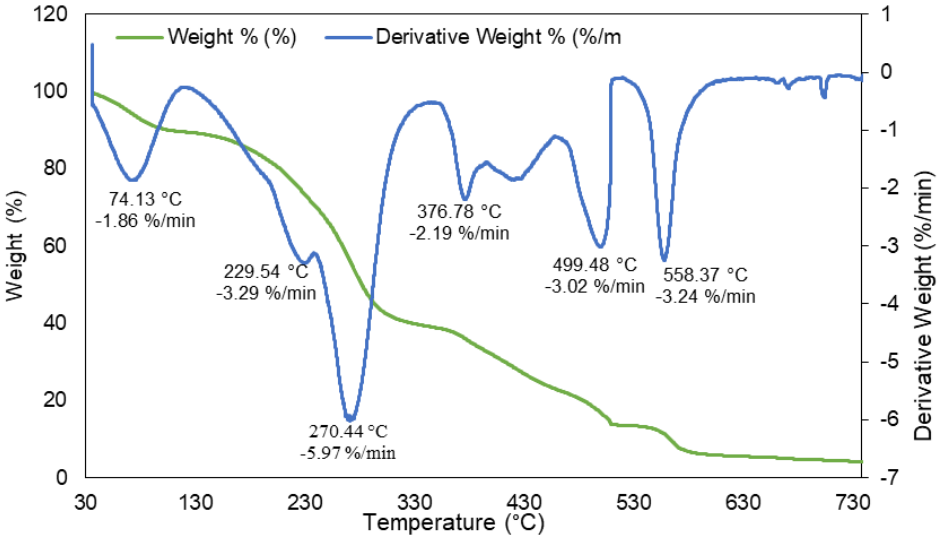

Fig. 8a. DTG of nanochitosan chlorhexidine film

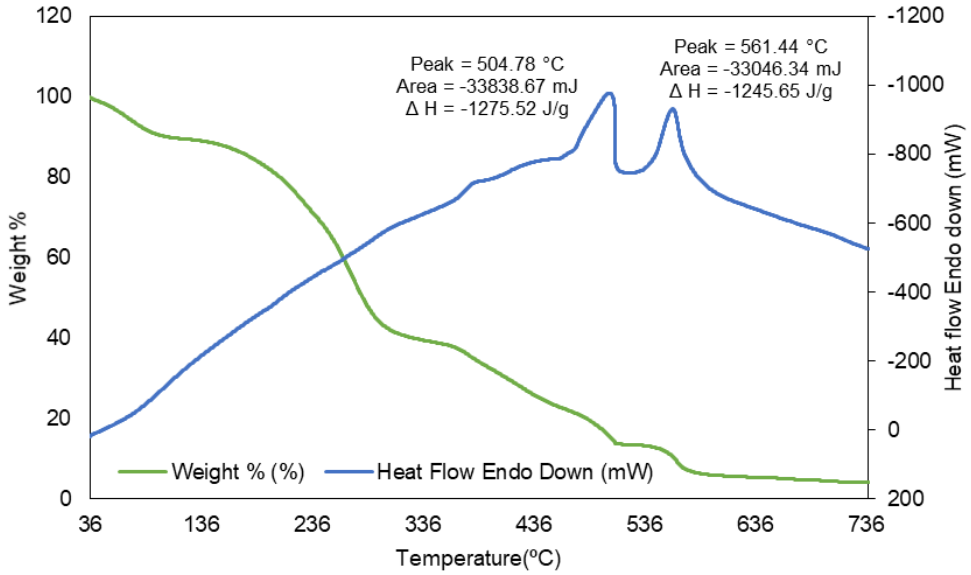

Fig. 8b. DTA of nanochitosan chlorhexidine film

Table 2. Moisture content and film solubility of the films

Functional tests	NC	NC-CLX
Moisture Content (MC) %	35.33±2.67	22.44±2.03
Film Solubility (%)	25.27±0.70[a]	12.96±0.73[b]

[a] and [b] indicates significance level at 5% using Independent t-test

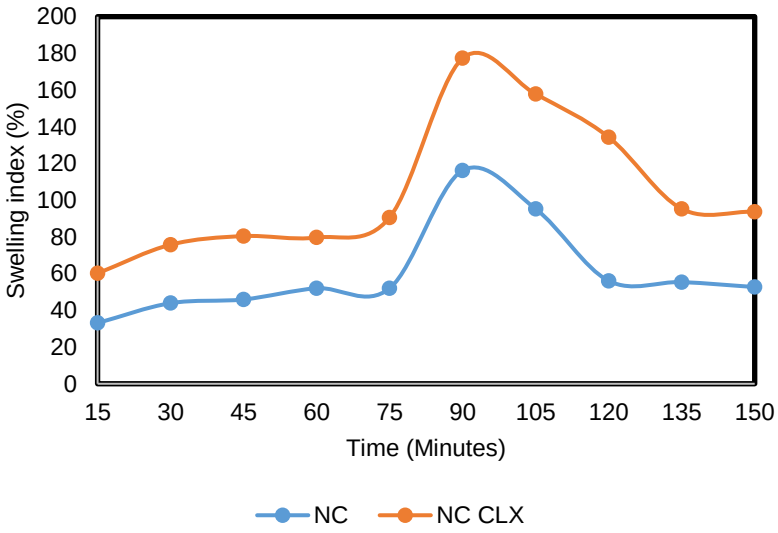

Fig. 9. Swelling Index of NC and NC-CLX Film

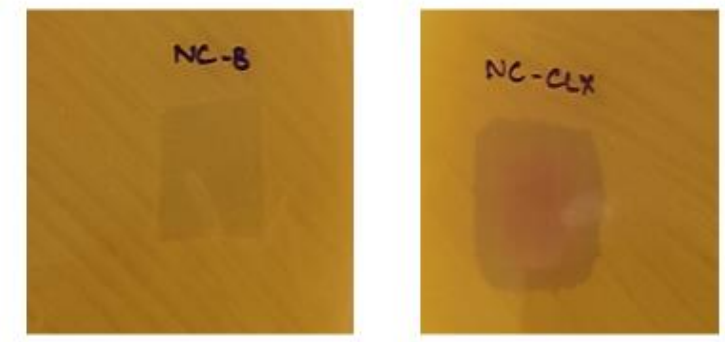

Fig. 10. Anti-bacterial activity NC and NC-CLX film

trend may be attributed to the robust interaction between phenolic compounds and the polysaccharide chain of chitosan, potentially diminishing the availability of amine and hydroxyl groups in the polymer for interaction with water. Consequently, the water solubility of the film decreased. In the realm of drug delivery and pharmaceutical applications, films with reduced solubility can be tailored to release active ingredients gradually and predictably. This controlled release mechanism ensures a consistent and sustained therapeutic effect, thereby enhancing patient compliance and treatment efficacy.

3.8.3 Swelling Index (Fluid handling capacity)

Swelling plays a crucial role in the evaluation of biodegradable films, influencing their water resistance, particularly in humid conditions [46]. The permeation of solvent into the chitosan polymer matrix induces the expansion of the composite membrane and causes localized relaxation of segments within the polymer matrix [19] ascertained by ionic repulsion mechanism. The higher swelling index of NC-CLX films indicates its fluid handling capacity at pH 7.4 (acute wound), which remain optimal for wound healing [46].

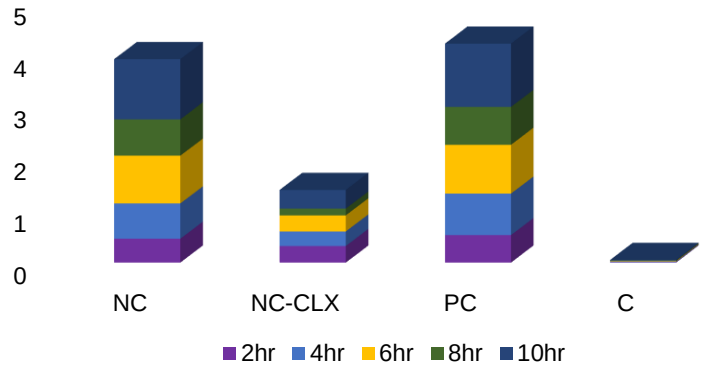

Fig. 11a. Modified growth inhibition assays for the NC and NC-CLX Films of *E. coli*

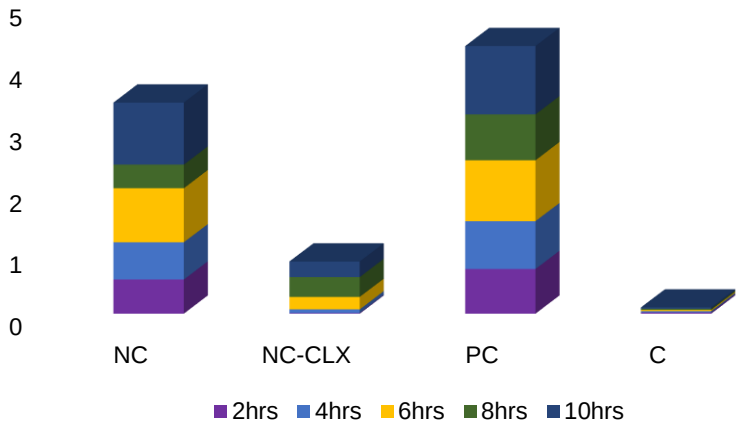

Fig. 11 b. Modified growth inhibition assays for the NC and NC-CLX Films of MRSA

3.9 Anti-Bacterial Activity

In this investigation nanochitosan (NC) and nanochitosan chlorhexidine (NC-CLX) films were employed. Significantly, films incorporating chlorhexidine displayed a discernible inhibition zone. Using a 0.5 McFarland Standard concentration of Methicillin-Resistant *Staphylococcus aureus* (MRSA) culture spread on Mannitol Salt agar (MSA), the films were placed over the bacterial culture. The observed inhibition zone hierarchy was NC-CLX > NC. The antimicrobial efficacy of nanochitosan, characterized by NH_3^+ groups, involves interaction with the negatively charged surface of microbial cell membranes. This interaction disrupted cell functions by breaking components or inhibiting cell activity, resulting in microbial cell death. Nano chitosan's capability to penetrate microbial cell membranes enables it to bind to DNA, hindering the synthesis of RNA, enzymes, and proteins [47]. Conversely, cationic chlorhexidine binds to the negatively charged cell wall of bacteria, attacking cell membranes and causing cell death [48]. The shift from traditional assays to micro-well-based assays is attributed to their simplicity, cost-effectiveness, and ability to analyses a larger sample volume in a shorter timeframe

In this study, modified growth inhibition assay (MGIA) was applied, utilizing 96-well microtiter plates to evaluate the active period of films concerning its applications to the wound. Both *Escherichia coli* and MRSA (wound associated

bacteria) were cultured in the 96-well plates for a period of 10 hours. Results obtained from the MGIA indicated that NC-CLX demonstrated a more robust antimicrobial activity compared to NC. The presence of the film impeded bacterial growth, evident from the reduction in optical density measurements. This inhibitory effect on bacterial growth was further supported by the sustained growth observed in the positive control wells, where only bacteria were present without the film. Conversely, the negative control wells, lacking both bacteria and the film, exhibited unaltered OD values. The findings of this study suggested that the NC-CLX film possessed superior antimicrobial properties as seen from Fig. 11a. and 11b. The use of MGIA in 96-well microtiter plates provided a convenient and effective method for evaluating the antimicrobial characteristics of the films. In accordance to the results, the NC-CLX films offered an active period of > 10 hrs. at experimental conditions.

4. CONCLUSION

In this investigation, nanochitosan composite films infused with chlorhexidine were formulated with the primary goal of amplifying their antimicrobial efficacy for wound healing applications. The intrinsic antibacterial attributes of chitosan, stemming from its primary amine groups, were fine-tuned through the incorporation of chlorhexidine. The films underwent thorough physiochemical analyses, encompassing XRD, SEM, FTIR, and TGA, to elucidate their characteristics. The amalgamation of chlorhexidine into nanochitosan films not only broadens their functional spectrum, including enhanced fluid handling capacity and resistance, but also bestows antimicrobial advantages, biocompatibility, and the potential for multifunctional properties. This unique combination positions these films as a highly promising option for wound care and diverse therapeutic applications in the medical and healthcare domains.

ACKNOWLEDGEMENTS

The authors acknowledge the Director, Indian Council of Agricultural research-Central Institute of Fisheries Technology (ICAR-CIFT), Cochin, Kerala, India for providing the facilities to carry out this work and also for granting permission to publish the data acquired from the study. The authors would like to express their sincere gratitude to ICAR for providing funds to carry out the research work under ICAR-National Fellow Scheme and Sophisticated Test & Instrumentation Centre, Cochin University of Science and Technology, Cochin for carrying out various analyses.

COMPETING INTERESTS

Authors have declared that no competing interests exist.

REFERENCES

1. Davies P, Stephenson J, Manners C. Understanding undisturbed wound healing in clinical practice—a global survey of healthcare professionals. Wounds International. 2019;*10*(2):50-57.
2. Nguyen HM, Le TTN, Nguyen AT, Le HNT, Pham TT. Biomedical materials for wound dressing: Recent advances and applications. RSC Advances. 2023;13(8), 5509-5528.
3. Amruth P, Rosemol Jacob M, Paul PT, Anandan R, Mathew S. Ideal properties of carrageenan-based films for wound healing applications. Journal of Experimental Zoology India, 2022;25(1) 565-570.
4. Sah AK, Dewangan M, Suresh PK. Potential of chitosan-based carrier for periodontal drug delivery. Colloids and Surfaces B: Biointerfaces. 2019; 178:185-198.
5. Amruth P, Rosemol Jacob M, Suseela Mathew and Anandan R. Developmental prospectives of new generation super absorbent wound dressing materials from sulfated polysaccharide of marine red algae Journal of the University of Shanghai for Science and Technology. 2021;23(9): 400-408
6. Amruth P, Rosemol Jacob M, Joy JM, Anandan R, Mathew S*. In vivo* evaluation of wound healing efficacy of κ -Carrageenan blended polyvinyl pyrrolidinone films for wound dressing applications. International Journal of Zoology and Applied Biosciences. 2023;8(4):16-20
7. Boateng JS, Pawar HV, Tetteh J. Polyox and carrageenan based composite film dressing containing anti-microbial and anti-inflammatory drugs for effective wound healing. International journal of pharmaceutics. 2013;441(1-2):181-191.
8. Sedayu BB, Cran MJ, Bigger SW. A review of property enhancement techniques for carrageenan-based films and coatings. Carbohydrate Polymers. 2019; 216:287-302.

9. Hajji S, Ktari N, Ben Salah R, Boufi S, Debeaufort F, Nasri, M. Development of nanocomposite films based on chitosan and gelatin loaded with chitosan-tripolyphosphate nanoparticles: antioxidant potentials and applications in wound healing. Journal of Polymers and the Environment. 2021;30:833–854
10. Iliou K, Kikionis S, Ioannou E, Roussis, V. Marine biopolymers as bioactive functional ingredients of electrospun nanofibrous scaffolds for biomedical applications. Marine Drugs. 2022;20(5):314.
11. Oryan A, Sahvieh S. Effectiveness of chitosan scaffold in skin, bone and cartilage healing. International Journal of Biological Macromolecules. 2017; 104:1003-1011.
12. Srinivasa PC., Ramesh, MN, Kumar KR, Tharanathan RN. Properties and sorption studies of chitosan–polyvinyl alcohol blend films. Carbohydrate Polymers. 2003;53(4), 431-438
13. Ma Y, Xin L, Tan H, Fan M, Li J, Jia Y, Hu X. Chitosan membrane dressings toughened by glycerol to load antibacterial drugs for wound healing. Materials Science and Engineering: C. 2017; 81:522-531.
14. Varoni E, Tarce M, Lodi G, Carrassi A. Chlorhexidine (CHX) in dentistry: state of the art. Minerva Stomatol. 2012;61(9):399-419.
15. Onnainty R, Onida B, Páez P, Longhi M, Barresi A, Granero G. Targeted chitosan-based bionanocomposites for controlled oral mucosal delivery of chlorhexidine. International Journal of Pharmaceutics. 2016;509(1-2):408-418.
16. Ramezani Z, Zarei M, Raminnejad N. Comparing the effectiveness of chitosan and nanochitosan coatings on the quality of refrigerated silver carp fillets. Food Control. 2015; 51:43-48.
17. Rosemol Jacob M, Amruth P, Akshay P, Stephy Rose KV, Anandan R, Suseela Mathew In vivo assessment of wound closure and biocompatibility of nanochitosan-polyvinylalcohol-glycerol films in experimental animal model. International Journal of Zoology and Applied Biosciences. 2023;8(6):77-83.
18. Bahrami S, Esmaeilzadeh S, Zarei M, Ahmadi F. Potential application of nanochitosan film as a therapeutic agent against cutaneous leishmaniasis caused by L. major. Parasitology Research. 2015; 114(12):4617-4624
19. Dara PK, Raghavankutty M, Balaraman G, Ashraf PM, Visnuvinayagam S, Tejpal CS, Rangasamy A. Biocompatibility and histopathological evaluation of chitosan nanoparticles grafted fish gelatin bio-nanocomposite membranes in rats. Iranian Polymer Journal. 2021;30(9):953-964
20. Orsuwan A, Shankar S, Wang LF, Sothornvit R, Rhim JW. Preparation of antimicrobial agar/banana powder blend films reinforced with silver nanoparticles. Food Hydrocolloids. 2016; 60:476-485.
21. Visnuvinayagam S, Murthy LN, Jeyakumari A, Parvathy U, Anandan R, Sivaraman GK, Ravishankar CN. Combined effect of zinc oxide nano particle incorporated chitosan for better antimicrobial activity towards wound healing. Journal of Environmental Biology. 2019;40.691-697
22. Sterniša M, Sabotič J, Klančnik A. A novel approach using growth curve analysis to distinguish between antimicrobial and anti-biofilm activities against Salmonella. International journal of food microbiology. 2022;364:109520
23. Asgarirad H, Ebrahimnejad, P., Mahjoub, M. A., Jalalian, M., Morad, H., Ataee, R., ... & Farmoudeh A. A promising technology for wound healing; in-vitro and in-vivo evaluation of chitosan nano-biocomposite films containing gentamicin. Journal of Microencapsulation. 2021;38(2):100-107
24. Huang KS, Sheu YR, Chao IC. Preparation and properties of nanochitosan. Polymer-Plastics Technology and Engineering. 2009;48(12):1239-1243.
25. Alehosseini E, Shahiri Tabarestani H, Kharazmi MS, Jafari SM. Physicochemical, Thermal, and Morphological Properties of Chitosan Nanoparticles Produced by Ionic Gelation. Foods. 2022;11(23):3841.
26. Oliveira Lima K, Barreto Pinilla CM, Alemán A, López-Caballero ME, Gómez-Guillén MC, Montero P, Prentice C. Characterization, bioactivity and application of chitosan-based nanoparticles in a food emulsion model. Polymers. 2021;13(19):3331.
27. Raval N, Maheshwari R, Kalyane D, Youngren-Ortiz SR, Chougule MB, Tekade RK. Importance of physicochemical characterization of nanoparticles in pharmaceutical product development. In Basic fundamentals of drug delivery Academic Press. 2019;369-400
28. Ding X, Zhao L, Khan IM, Yue L, Zhang Y, Wang Z. Emerging chitosan grafted essential oil components: A review on

synthesis, characterization, and potential application. Carbohydrate Polymers. 2022; 120011.
29. Santana Neto MC, Costa MLVDA, Fialho PHDS, Lopes GLN, Figueiredo KA, Pinheiro IM, Carvalho ALM. Development of chlorhexidine digluconate and Lippia sidoides essential oil loaded in microemulsion for disinfection of dental root canals: Substantivity profile and antimicrobial activity. AAPS PharmSciTech. 2020; 21:1-11.
30. Vijayalakshmi K, Devi BM, Sudha PN, Venkatesan J, Anil S. Synthesis, characterization and applications of nanochitosan/sodium alginate/microcrystalline cellulose film. J. Nanomed. Nanotechnol. 2016;7(6):419.
31. Ferreira MOG, de Lima IS, Morais AÍS, Silva SO, de Carvalho RBF, Ribeiro AB, Silva Filho EC. Chitosan associated with chlorhexidine in gel form: Synthesis, characterization and healing wounds applications. Journal of Drug Delivery Science and Technology. 2019;49: 375-382.
32. Zolfi M, Khodaiyan F, Mousavi M, Hashemi M. Development and characterization of the kefiran-whey protein isolate-TiO2 nanocomposite films. International Journal of Biological Macromolecules. 2014; 65:340-345.
33. Vinodhini PA, Sangeetha K, Thandapani G, Sudha PN, Jayachandran V, Sukumaran A. FTIR, XRD and DSC studies of nanochitosan, cellulose acetate and polyethylene glycol blend ultrafiltration membranes. International Journal of Biological Macromolecules. 2017; 104:1721-1729.
34. Ma IW, Sh A, Ramesh K, Vengadaesvaran B, Ramesh S, Arof AK. Anticorrosion properties of epoxy-nanochitosan nanocomposite coating. Progress in Organic Coatings. 2017; 113:74-81.
35. Meera K, Arun K, Ramesan MT. nanochitosan reinforced polyvinyl alcohol/cashew gum bio-blend nanocomposites: promising materials for future frontiers. Journal of Polymers and the Environment. 2023;31:4487–4505
36. Rajeshwari K, Gomathi T, Sudha PN. Synthesis and characterization of nanochitosan-polyvinyl alcohol-carboxymethyl starch ternary blends of various compositions with glutaraldehyde as crosslinking agent. World Journal of Pharmaceutical Research. 2017;7(8):533-549
37. Lobato-Aguilar H, Uribe-Calderón JA., Herrera-Kao W, Duarte-Aranda S, Baas-López JM, Escobar-Morales B, Cervantes-Uc JM. Synthesis, characterization and chlorhexidine release from either montmorillonite or palygorskite modified organoclays for antibacterial applications. Journal of Drug Delivery Science and Technology. 2018; 46:452-460.
38. Shakour N, Khoshkhoo Z, Akhondzadeh Basti A, Khanjari A, Mahasti Shotorbani P. Investigating the properties of PLA-nanochitosan composite films containing Ziziphora Clinopodioides essential oil and their impacts on oxidative spoilage of Oncorhynchus mykiss fillets. Food Science & Nutrition. 2021;9(3):1299-1311.
39. Cazón P, Velázquez G, Vázquez M. Characterization of bacterial cellulose films combined with chitosan and polyvinyl alcohol: Evaluation of mechanical and barrier properties. Carbohydrate Polymers. 2019;216:72-85
40. Chopra H, Bibi S, Kumar S, Khan MS, Kumar P, Singh I. Preparation and evaluation of chitosan/PVA based hydrogel Films Loaded with honey for wound healing application. Gels. 2022;8(2):1-21.
41. Tomás I, Rubido S, Donos N. In situ antimicrobial activity of chlorhexidine in the oral cavity. Sci. against Macrobial Pathog. Comminicating Curr. Res. Thechnological Adv., A. Mendez-Vilas, Ed., Formatex. 2011;530-541.
42. Díez-Pascual AM, Díez-Vicente AL. Wound healing bionanocomposites based on castor oil polymeric films reinforced with chitosan-modified ZnO nanoparticles. Biomacromolecules. 2015;16(9):2631-2644
43. Mohanty C, Sahoo SK. Curcumin and its topical formulations for wound healing applications. Drug discovery today. 2017; 22(10):1582-1592.
44. Sadiq T, Khalid SH, Khan IU, Mahmood H, Asghar S. Designing Deferoxamine-Loaded Flaxseed Gum and Carrageenan-Based Controlled Release Biocomposite Hydrogel Films for Wound Healing. Gels. 2022; 8(10):652
45. Abdul-Rahman SM, Abass AF. Preparation of edible films made from chitosan with pomegranate peel extract and study its barrier, mechanical and antioxidant properties. In IOP Conference Series: Earth

and Environmental Science. IOP Publishing. 2021;761(1):012122
46. Peng Y Li Y. Combined effects of two kinds of essential oils on physical, mechanical and structural properties of chitosan films. Food Hydrocolloids. 2014;36:287-293
47. Ngo TMP, Nguyen TH, Dang TMQ, Tran TX, Rachtanapun P. Characteristics and antimicrobial properties of active edible films based on pectin and nanochitosan. International journal of molecular sciences. 2020; 21(6):2224.
48. Viswanathan K, Monisha P, Srinivasan M, Swathi D, Raman M, Raj GD. (Chlorhexidine-calcium phosphate nanoparticles—polymer mixer based wound healing cream and their applications. Materials Science and Engineering: C. 2016; 67:516-521.

Peer-review history:
The peer review history for this paper can be accessed here:
https://www.sdiarticle5.com/review-history/113723